

Deflection of Neutral Molecules using the Nonresonant Dipole Force

H. Stapelfeldt,^{1,*} Hirofumi Sakai,^{1,2} E. Constant,^{1,3} and P. B. Corkum¹

¹Steele Institute for Molecular Sciences, National Research Council of Canada, Ottawa, Ontario, Canada K1A 0R6

²Electrotechnical Laboratory, 1-1-4, Umezono, Tsukuba, Ibaraki 305, Japan

³Département de Physique, Faculté des Sciences, Université de Sherbrooke, Sherbrooke, Québec, Canada J1K 2R1

(Received 3 April 1997)

The ac Stark shift produced by nonresonant radiation creates a potential minimum for a ground state molecule at the position where the laser intensity is maximum. The gradient of this potential exerts a force on the molecule. We experimentally observe this force when a beam of CS₂ molecules is redirected by sending it through the intensity gradient near the focus of a laser beam. We trace the direction of the molecules in the molecular beam, showing that the molecules that pass near the center of the high intensity laser beam will focus. [S0031-9007(97)04209-9]

PACS numbers: 42.50.Vk, 33.80.Ps, 51.70.+f

The use of laser light to manipulate and control the position and velocity of electrons [1], atoms [2], and microscopic particles [3,4] is a subject of intense activity in physics and biology. The manipulation of atoms in the gas phase is based on either the scattering force, exploited in most laser cooling techniques [5], or the induced dipole force. In the latter case a dipole moment is induced in the atom using a near-resonant continuous-wave laser beam. The polarized atoms experience a force that is proportional to the spatial gradient of the laser intensity, which can be used, for instance, to focus [6] or trap them [5].

The powerful laser cooling and trapping techniques developed for atoms are not readily applicable to molecules, due to their complicated level structure and their weak transition moments for any given rovibrational transition. Consequently, laser manipulation and control of neutral particles beyond the atomic case has been restricted to biological molecules in solution [4] and small dielectric particles [3]. Manipulation and control of molecules in the gas phase, however, remains a topic of great interest [7,8].

We use the nonresonant molecular polarizability to exert an induced dipole force that modifies the trajectory of gas phase molecules. By sending a beam of molecules through the focus of a laser beam oriented perpendicularly to their direction of propagation, we observe a change of the transverse velocity of the molecules. The velocity change is proportional to the spatial gradient of the laser intensity. We demonstrate that an intense laser beam can be used as a lens to focus the molecular beam.

Using nonresonant polarizability and intense laser fields, we solve two problems that have impeded the development of molecular optics. First, we remove the restrictions caused by the dense level structure of the molecule by using far-off resonance radiation to induce a dipole force. In this way, there is no critical dependence on the particular level structure of the molecule. Therefore, our approach is applicable to all molecules (or atoms [9]). Second, by employing the intense field from a pulsed laser to induce the molecular dipole moments, we obtain light-induced forces that are many orders of magnitude larger

than the forces induced on atoms by standard continuous-wave laser beams. This allows manipulation of molecules without laser cooling [10].

For experimental convenience, we use a molecular beam to produce molecules that are translationally cold in the direction perpendicular to the jet axis. Our experiment is designed to observe changes in the transverse velocity (deflection) against this very cold background. We will show potential well depths of about 7.0 meV, approximately 4 orders of magnitude greater than the transverse beam energy (10⁻⁶ eV).

The schematic of the experimental layout is shown in Fig. 1. A pulsed beam of CS₂ molecules is formed by expanding a CS₂ gas at ~25 Torr, either buffered with 1 atm of neon or without the neon buffer, through a 250- μ m-diameter nozzle into a time-of-flight (TOF) spectrometer with the molecular beam axis (the x axis) perpendicular to the TOF axis (the y axis). The molecules travel freely for ~8 cm, after which they are crossed at 90° by the focused beam from a pulsed (10 Hz) Nd:YAG laser ($\lambda = 1.06 \mu\text{m}$) propagating along the z axis. The duration of the YAG pulse is 14 ns (FWHM). We use

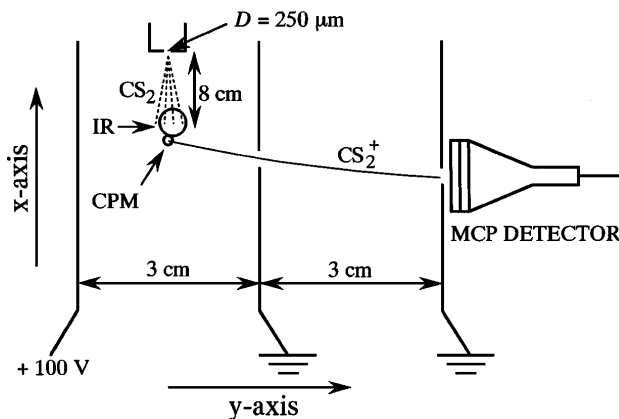


FIG. 1. Schematic of the experimental arrangement of the target chamber viewed in the direction of the laser beam (z axis).

laser pulses with energy in the range of 10 mJ. The laser beam is focused with an on-axis parabolic mirror to an $\omega_0 = 7 \mu\text{m}$ Gaussian focal spot giving a peak intensity of $I_0 \sim 9 \times 10^{11} \text{ W/cm}^2$ at 10 mJ.

This laser field exerts an induced dipole force on the CS_2 molecules, which causes a change in the velocity of the molecules. We measure the velocity change [11] along the TOF axis—i.e., perpendicular to the molecular velocity before the interaction. To do this we multiphoton ionize the neutral molecules using a tightly focused femtosecond laser beam ($\lambda = 625 \text{ nm}$) and observe the distribution of flight times of the CS_2^+ ions from the interaction region to the microchannel plate detector (illustrated in Figs. 1 and 2). The TOF mass spectrometer [11] consisted of an acceleration region defined by two plates and an equal length field-free drift region (Fig. 1). With this design, molecular ions with their transverse velocity component towards the detector at the time of ionization arrive before zero-transverse velocity ions. Those initially deflected away from the detector arrive after zero-transverse velocity ions.

The 80 femtosecond duration pulses, originating from a 10 Hz amplified colliding pulse mode-locked (CPM) laser, contain $0.66 \mu\text{J}$ per pulse and are focused to a spot size $\omega_0 \sim 2.5 \mu\text{m}$ that corresponds to a peak intensity of $8 \times 10^{13} \text{ W/cm}^2$. To ensure that ionization occurred without the strong infrared pulse present, a 25 ns delay is introduced between the YAG pulse and the CPM pulse (requiring a corresponding $10 \mu\text{m}$ offset in the direction of the molecular beam velocity in the position of their focal spots for pure CS_2 , $20 \mu\text{m}$ for CS_2 buffered with neon). The nonlinearity of multiphoton ionization allows

us to restrict the probe volume to a region smaller than the YAG focal volume by adjusting the focal spot size as well as the intensity of the CPM laser beam. Therefore, we can use the CPM laser to probe the spatial dependence of the induced dipole force simply by moving its focus with respect to the larger YAG focus.

Examples of the relevant portions of three TOF spectra are shown in Fig. 2. Each spectrum is the average of 1000 shots. The central (full) curve, recorded without the YAG laser present, gives information on the initial velocity distribution along the y axis of the molecular beam. Since our velocity measurement is restricted to those molecules that pass through the very small focal spot of the CPM laser, we expect the distribution to be very narrow. In fact, simple line-of-sight arguments show that the initial velocity spread along the y axis, Δv_y^{init} , is determined by $\Delta v_y^{\text{init}} = D/(l/v_{\text{CS}_2})$, where $D = 250 \mu\text{m}$ is the diameter of the nozzle, $l = 8 \text{ cm}$ is the distance from the nozzle to the laser focus, and v_{CS_2} is the longitudinal velocity of the CS_2 molecules. For the unbuffered (buffered) expansion we measured $v_{\text{CS}_2} = 450$ (800 m/s). At this velocity, the CS_2 molecules therefore have a transverse velocity spread of $\sim 1.4 \text{ m/s}$ ($\sim 2.5 \text{ m/s}$) equivalent to a kinetic energy of $0.8 \times 10^{-6} \text{ eV}$ ($2.5 \times 10^{-6} \text{ eV}$). In Fig. 2 the CS_2 molecules are not buffered with neon during the expansion. The FWHM of the full peak ($\sim 3.4 \text{ ns}$) corresponds to a y -axis velocity spread of 7.2 m/s , which is significantly larger than the expected value of $\sim 1.4 \text{ m/s}$. Thus, it provides a calibration of our ability to measure transverse velocities with the TOF spectrometer.

The remaining two spectra in Fig. 2 were obtained for molecules that transmit the focus of the YAG laser (peak intensity = $1 \times 10^{12} \text{ W/cm}^2$, linear polarization) prior to the measurement of their velocity by the CPM laser. They were obtained for molecules that pass approximately $3.5 \mu\text{m}$ to the right of the center of the YAG focus (dotted curve in Fig. 2) and to the left of the center of the YAG focus (dashed curve in Fig. 2), respectively. The molecules arriving earlier at the detector (dashes) have acquired a y -axis velocity towards the microchannel plate detector [11]. Similarly, the molecules arriving later at the detector (dots) have acquired a negative y -axis velocity component from the YAG laser pulse. As expected, the laser-induced dipole force provides a central potential deflecting the molecules towards the high intensity region.

By recording TOF spectra of molecules for several positions of the CPM focus with respect to the YAG focus, we can measure the detailed y -coordinate dependence of the velocity change [11], and therefore of the dipole force. This is implemented by scanning the YAG focus over a range of $\sim 30 \mu\text{m}$ while keeping the CPM focus fixed. In this way, the ions produced by the CPM laser always originate from the same spatial location, ensuring that the observed changes in the TOF spectra are not caused by the position of the ionizing laser inside the TOF spectrometer. The results are displayed in Fig. 3, where the velocity shift

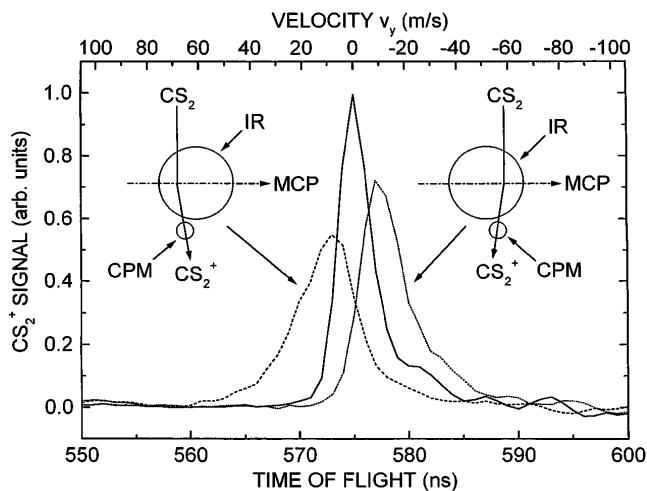


FIG. 2. Portion of the time-of-flight spectrum showing the time of arrival of the undeflected beam (solid curve) and the deflected beams (dashed and dotted curves). A schematic shows the relative placement of the focus of the deflecting laser (YAG) and the measurement laser (CPM). Deviations of the arrival time of a deflected molecule from the arrival time of a zero transverse velocity molecule allow the transverse velocity to be measured. The horizontal scale shows both the flight time and the transverse velocity v_y .

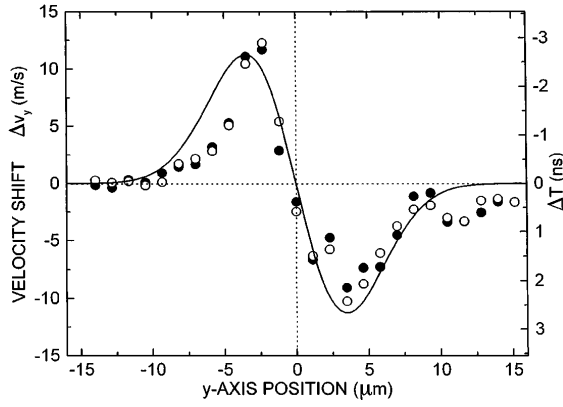


FIG. 3. The shift in arrival time ΔT induced by the dipole force and the associated transverse velocity Δv_y of the molecular beam plotted as a function of the position of the molecule that is probed in the focus of the deflecting laser beam. Data obtained with the deflection laser linearly polarized is represented by the symbol \bullet ; data obtained with circular polarization is represented by \circ . In both cases, the expansion of CS_2 molecules was buffered with neon. The derivative of the measured focal distribution of the deflecting laser beam is also shown by the solid curve.

of the center of the half maximum CS_2^+ signal is plotted as a function of the y coordinate of the YAG laser focus for both linear and circular polarization. The dispersionlike shape shows that the force causing the velocity change [Eq. (2)] is proportional to the y derivative of the YAG laser intensity profile (solid curve). (Deviations on the right of Fig. 3 experimental data and the y derivative of the intensity profile are due to space charge caused by ionization of CS_2 by the YAG beam [12].)

Those molecules that pass near the center of the focus (within $\pm\omega_0/2$) experience a displacement that causes them to meet at a common position; that is, the beam will focus. The focal length of our molecular lens is approximately $230 \mu\text{m}$, corresponding to a redirection of the CS_2 molecules through an angle of up to 0.9° . The lens is thin since the size of the YAG beam is much smaller than the focal length.

We can estimate the magnitude of the potential well produced by the laser field for the CS_2 molecules. When a molecule enters the YAG laser focus, a dipole moment is induced. This results in a Stark shift U of the ground state of the molecule given by [13]

$$U(x, y, z, t) = -\frac{1}{4}\alpha E^2(x, y, z, t), \quad (1)$$

where $E(x, y, z, t)$ is the space and time dependent pulse envelope. Equation (1) includes a time average over one optical period and neglects alignment of the molecule by averaging over all angles [$\alpha = (\alpha_{\parallel} + 2\alpha_{\perp})/3$, where $\alpha_{\parallel, \perp}$ is the polarizability parallel and perpendicular to the molecular axis]. Using the static polarizability [14], Eq. (1) predicts a Stark shift $U_0 = 10 \text{ meV}$ at the center of the laser focus and at the peak of a laser pulse with $I = 9 \times 10^{11} \text{ W/cm}^2$. In comparison, typical potential

depths reached in continuous-wave studies on atoms are about $1 \mu\text{eV}$ [2,8].

We can approximately neglect alignment if we use either circularly polarized light (where the molecule can align only to a plane) or, linearly polarized light when the orientational well depth [$U_{\text{al}} = \frac{1}{4}(\alpha_{\parallel} - \alpha_{\perp})E^2$] is smaller than the rotational energy. Although U_{al} should be much greater than the estimated rotational temperature ($\approx 5 \text{ K}$) [15] of our jet cooled molecules, alignment does not play a significant role in our experiment. We reach this conclusion by comparing the deflection with linearly and circularly polarized light. If the molecules substantially align with the field, the deflection should be greater with linearly polarized light since then $U = -\frac{1}{4}\alpha_{\parallel}E_0^2$ and α_{\parallel} is always larger than the averaged α . Figure 3 compares the results obtained with linearly (solid circles) and circularly (open circles) polarized light. The lack of alignment may be due to our multilongitudinal mode YAG laser. Mode beating can produce transient spikes as short as 30 ps which is comparable to or even shorter than the rotational period τ_{rot} of the CS_2 molecules ($\tau_{\text{rot}} \sim 34 \text{ ps}$ for a rotational quantum number $J = 4$). Under these conditions alignment is not efficient [7]. By contrast, laser-induced alignment has been reported [16] when temporally smooth nanosecond laser pulses are used.

We now determine the maximum Stark shift $|U_0|$ from the experimental deflection data. Since the induced dipole force F exerted on a molecule is equal to $-\nabla U$, Eq. (1) shows that F is proportional to the gradient of the intensity. The YAG beam can be approximated by a Gaussian intensity distribution in both space and time: $I(x, y, z, t) = I_0 \exp[-2(x^2 + y^2)/\omega_0^2] \exp(-4 \ln 2 t^2/\tau^2)$ (we probe near $z = 0$). Therefore, the y component of the dipole force F_y is given by $F_y = -4(U_0/\omega_0^2)y \exp\{-2[(v_{\text{CS}_2}t)^2 + y^2]/\omega_0^2\} \exp[-4 \ln 2 t^2/\tau^2]$, where x has been replaced with $-v_{\text{CS}_2}t$ to describe the motion of the molecules along the x axis. The experimentally observed velocity shift Δv_y is related to F_y by $\Delta v_y = \frac{1}{m} \int_{-\infty}^{\infty} F_y(t) dt$ yielding

$$\Delta v_y = -4 \frac{\sqrt{\pi} U_0}{\sqrt{2} m \omega_0 v_{\text{CS}_2}} \times \frac{1}{\sqrt{1 + 2 \ln 2 (\frac{\omega_0/v_{\text{CS}_2}}{\tau})^2}} y \exp(-2y^2/\omega_0^2), \quad (2)$$

where m is the mass of the deflected molecule. The dispersionlike shape of the data points in Fig. 3 is consistent with the above expression for Δv_y . For reference, we plot the derivative of the measured spatial profile of the YAG beam on the same figure (determined by measuring a 20 times magnified image of the focus).

The maximum Stark shift U_0 can be estimated from the experimental measurements. Solving Eq. (2) for U_0 at $y = \omega_0/2$, where the measured $\Delta v_y = 12 \text{ m/s}$, yields

$U_0 = 6.2$ meV. This agrees with the calculated value ($U_0 = 10$ meV) within experimental uncertainty in measuring the pulse duration, energy, focal properties, and the longitudinal velocity of the CS₂ molecules.

The maximum intensity that an atom or molecule can withstand without substantial multiphoton ionization determines the maximum Stark shift that can be obtained. At sufficiently long wavelength and high intensity light, ionization can be accurately calculated as tunneling [17]. Applying tunnel ionization formulas [17] to CS₂, with its ionization potential of 10.1 eV, we find 1% probability of ionization during a 10 ns pulse (ionization rate $\rho = 10^6$ s⁻¹) at an intensity of 8×10^{12} W/cm² ($U_0 = 90$ meV). Since multiphoton ionization is a very nonlinear function of the intensity, 8×10^{12} W/cm² is an effective threshold intensity for CS₂.

In our experiment, ionization becomes important at a much lower peak laser intensity for two reasons. First, 1.06 μ m irradiation of CS₂ does not satisfy the conditions for tunnel ionization [17]. Typically, nontunneling processes raise the ionization rate and therefore lower the peak intensity at which significant ionization is reached. Second, the high-intensity spikes of the YAG pulse limit the average intensity that can be employed before multiphoton ionization occurs as compared to the situation with a temporally smooth pulse.

Assuming tunneling, the maximum Stark shift on any neutral atom or small molecule is approximately constant, although the polarizability can vary greatly. As the polarizability α decreases, the ionization potential increases and the maximum intensity ($\propto E^2$) that the molecule can withstand without ionization [17] roughly compensates for the decreasing polarizability [see Eq. (1)]. For example, the Stark shift of H₂, a very unpolarizable molecule, is 50 meV at an intensity where the tunnel ionization rate reaches 10^6 s⁻¹.

In conclusion, through nonresonant molecular polarizability, large forces can be applied to molecules. Controlling the laser radiation means controlling the external molecular coordinates. Our results point to a method for trapping, focusing, wave guiding, accelerating, or decelerating molecules. In short, many aspects of atomic optics can be transferred to molecular optics by using nonresonant intense fields. It appears that manipulation of molecules without significant reduction of their thermal temperature is within reach.

We acknowledge the technical assistance of B. Avery, D. Joines, and D. Roth. Discussions with M. Yu. Ivanov, T. Seideman, and A. Stolow are also acknowledged

as well as the careful reading of the manuscript by M. Drewsen.

*Present address: Department of Chemistry, Aarhus University, Langelandsgade 140, DK-8000 Aarhus C, Denmark.

- [1] P. H. Bucksbaum, D. Schumacher, and M. Bashkansky, *Phys. Rev. Lett.* **61**, 1182 (1988); J. Chaloupka *et al.* (to be published).
- [2] See, for example, D. J. Wineland, C. E. Weiman, and S. J. Smith, in *Atomic Physics 14*, AIP Conf. Proc. No. 323 (AIP, New York, 1994).
- [3] A. Ashkin, J. M. Dziedzic, J. E. Bjorkholm, and S. Chu, *Opt. Lett.* **11**, 288 (1986).
- [4] S. K. Svoboda and S. Block, *Annu. Rev. Biophys. Biomol. Struct.* **23**, 247 (1994); A. Ashkin and J. M. Dziedzic, *Science* **235**, 1517 (1987); T. T. Perkins *et al.*, *Science* **264**, 822 (1994).
- [5] For a review, see C. S. Adams and E. Riis, *Prog. Quantum Electron.* **21**, 1 (1997).
- [6] J. J. McClelland *et al.*, *Science* **262**, 877 (1993); C. Kurtstiefer *et al.*, in *Atomic Interferometry*, edited by P. R. Berman (Academic, New York, 1997), p. 177.
- [7] B. Friedrich and D. Herschbach, *Phys. Rev. Lett.* **74**, 4623 (1995); T. Seideman, *J. Chem. Phys.* **106**, 2881 (1997).
- [8] J. T. Bahns, W. C. Stwalley, and P. L. Gould, *J. Chem. Phys.* **104**, 9689 (1996).
- [9] J. Takekoshi and R. J. Kinze, *Opt. Lett.* **21**, 77 (1996); J. D. Miller, R. A. Cline, and D. J. Heinzen, *Phys. Rev. A* **47**, 4567 (1993).
- [10] Neutral molecules can also be manipulated with static fields, but the forces are much weaker than those obtained here. See N. F. Ramsey, *Molecular Beams* (Clarendon, Oxford, 1956).
- [11] H. Stapelfeldt, E. Constant, and P. B. Corkum, *Phys. Rev. Lett.* **74**, 3780 (1995).
- [12] H. Sakai *et al.* (to be published).
- [13] A. A. Radtzig and B. M. Smirnov, *Reference Data on Atoms, Molecules, and Ions* (Springer-Verlag, New York, 1985).
- [14] K. J. Miller, *J. Am. Chem. Soc.* **112**, 8543 (1990).
- [15] We did not measure the rotational temperature T_{rot} , but previous measurements under essentially identical experimental conditions yielded $T_{\text{rot}} \sim 5$ K; see D. T. Cramb, H. Bitto, and J. R. Huber, *Chem. Phys.* **96**, 8761 (1992).
- [16] W. Kim and P. M. Felker, *J. Chem. Phys.* **104**, 1147 (1996).
- [17] M. V. Ammosov, N. B. Delone, and V. P. Krainov, *Sov. Phys. JETP* **64**, 1191 (1986); P. Dietrich and P. B. Corkum, *J. Chem. Phys.* **97**, 3187 (1992).